Supplementary Information

Highly Stable Lithium Anodes from Recycled Hemp Textile

Zhiyu Wang,[‡ ab] Peng Zhang,[‡b] Shasha Chen,[bc] Ken Aldren S. Usman,[b] Dylan Hegh,[b] Robert Kerr,[b] Hongjie Zhang,[*a] Si Qin,[*b] Chuyang Zhang,[a] Dan Liu,[b] Xungai Wang,[b] Weiwei Lei,[b] Joselito M. Razal[*b]

a. College of Textiles and Apparel, Quanzhou Normal University, Quanzhou, Fujian, 362000, China

b. Institute for Frontier Materials, Deakin University, Waurn Ponds, Victoria, 3216, Australia

c. College of Chemistry and Molecular Sciences, Wuhan University, Wuhan 430072, P. R. China

*Corresponding authors: zhjie016@qztc.edu.cn (H. Zhang); si.qin@research.deakin.edu.au (S. Qin); joselito.razal@deakin.edu.au (J. M. Razal)

EXPERIMENTAL

Fabrication of hemp@Li anodes. All chemicals were obtained from Sigma-Aldrich and used without further purification (Sydney, Australia). Hemp fabric waste was recovered from Shanxi Greenland Textile Co., Ltd and washed with distilled water followed by ethanol. The hemp was then placed into a quartz tube for pre-oxidation and heated in air to 260 °C, at rate of 5 °C min^{-1} for 1 h, followed by carbonization by

heating under a nitrogen atmosphere at a rate of 10 °C min^{-1} to 950 °C for 1 h. Then, the carbonized hemp was dipcoated by submerging in a 10 mg ml^{-1} dispersion of ZnO nanoparticle in a mixture of water and ethanol (1:1 v/v), which can remain stable for at least 10 minutes after sonication. The step was repeated several (1–5 times) times to produce hemp@ZnO with different ZnO loadings. Molten Li was produced by heating metallic Li on a hot plate heating at 300 °C in an argon-filled glovebox with both water and oxygen level below < 1 ppm. The ZnO coated hemp was inserted into the molten Li to produce the hemp@Li. Finally, the hemp@Li was punched into electrodes with a diameter of 10 mm, which were used directly as anodes.

Characterization. The morphologies of the samples were examined by a scanning electron microscope (ZEISS Supra 55 SEM) operated at an accelerating voltage of 5 kV. Raman spectra was collected on a Renishaw inVia Raman Microscope using 514 nm excitation (Argon ion laser).

Electrochemical Measurements. CR2032-type coin cells were assembled in an argon-filled glove box with both water and oxygen level below <1 ppm. To standardize the testing, coin cells were assembled using a fixed amount of 40 μL of 1 M $LiPF_6$ dissolved in ethylene carbonate (EC)/diethyl carbonate (DEC) as electrolyte without any additives and Celgard 2400 as the separator. Lithium bis(trifluoromethanesulfonyl)imide (LiTFSI, 1 M) in (DOL)/(DME) with 1 wt.% $LiNO_3$ was used as ether-based electrolyte. The hemp@Li anodes were cut round electrodes (10 mm in diameter) and assembled into coin cells for testing. To study Li plating/stripping morphology, ZnO19-hemp@Li was used as the working electrode with commercial Li chip as counter and reference electrodes. For cycling stability tests, the symmetric cells were assembled with hemp@Li anodes or Li chip as the working electrode, and Li chips as counter and reference electrodes. The full cell was assembled using lithium iron phosphate (LFP) with a capacity loading of 1 and 4 mA h cm^{-2} as cathodes, and hemp@Li or Li chips (rolled into ~300 μm for fair comparison) respectively as counter and reference electrodes. Electrochemical impedance spectroscopy

(EIS) measurements were performed on a Bio-Logic VMP-300 electrochemical workstation with an amplitude of 10 mV in the frequency range of 100 kHz to 10 mHz.

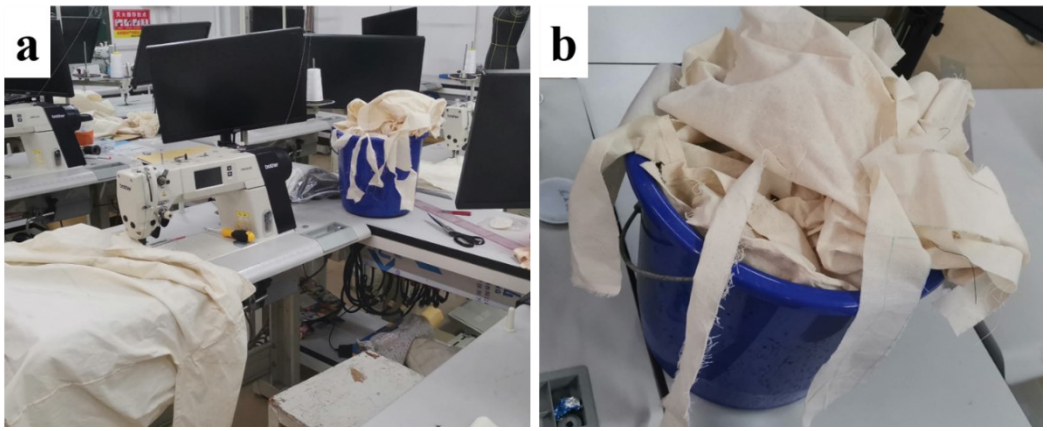

Fig. S1 Photo of waste hemp textile collected from industrial offcuts.

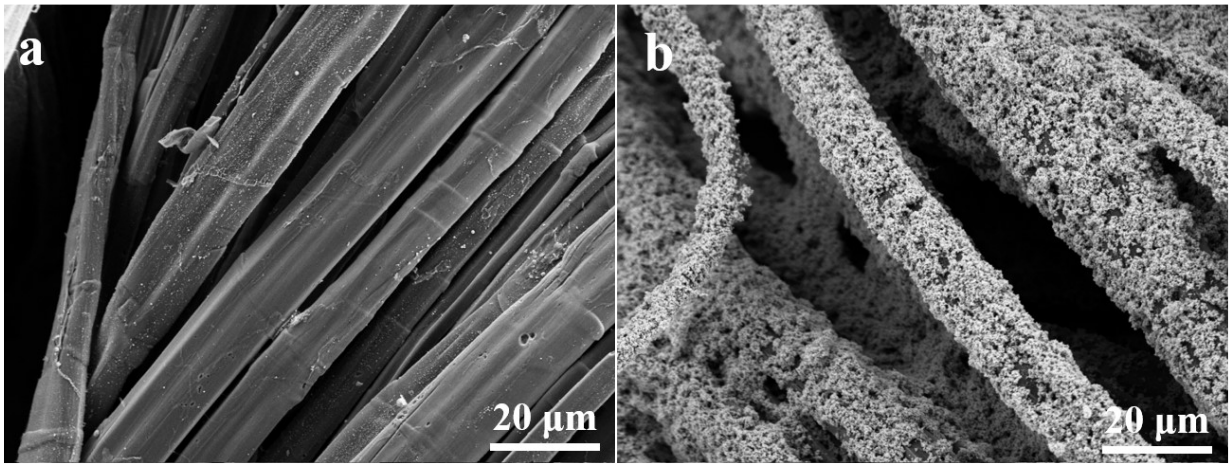

Fig. S2 High resolution SEM images of pure carbonized hemp textile (a) and carbonized hemp textile coated with 19% ZnO particles (b).

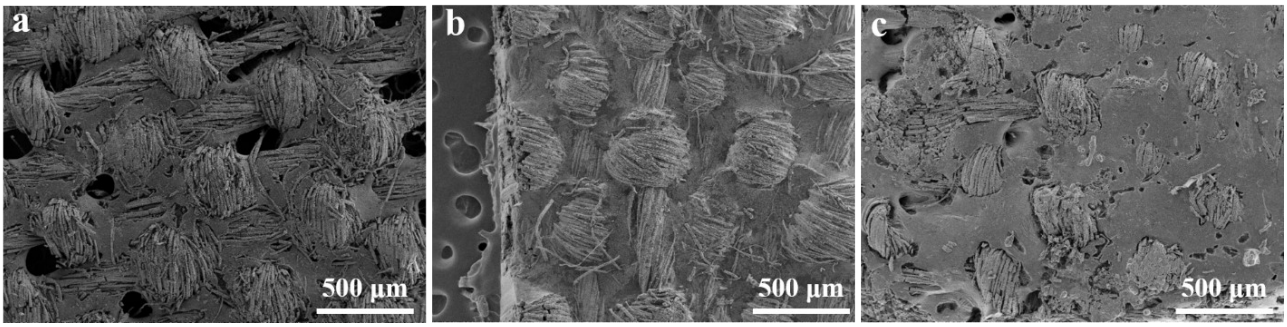

Fig. S3 SEM images of Li infused carbonized hemp fabric with ZnO loading of 4.5% (a), 10% (b) and 39% (c). It can be seen that carbonized hemp textile with a low ZnO loading of 4.5% and 10% shows limited lithiophilicity, leading to uneven distribution of infused Li, especially at a ZnO loading of 4.5%. However, the high loading of 39% led to uneven distributed pores and voids in ZnO39-hemp@Li.

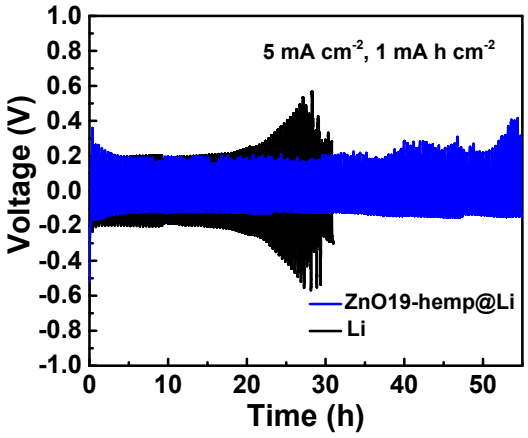

Fig. S4 Cycling stability of ZnO19-hemp@Li and neat Li anode at 5 mA cm^{-2} for 1 mA h cm^{-2}.

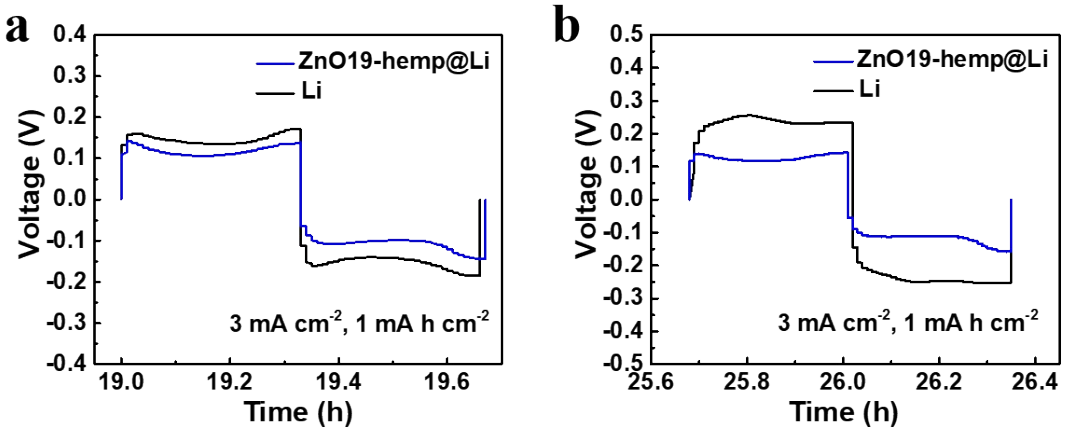

Fig. S5 Li plating and stripping profile of ZnO19-hemp@Li and pure Li chips at 3 mA cm^{-2} for 1 mA h cm^{-2}.

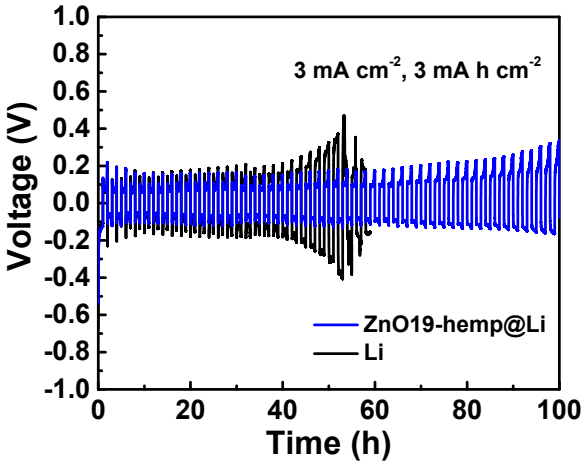

Fig. S6 Cycling stability of ZnO19-hemp@Li and neat Li anode at 3 mA cm^{-2} for 3 mA h cm^{-2}.

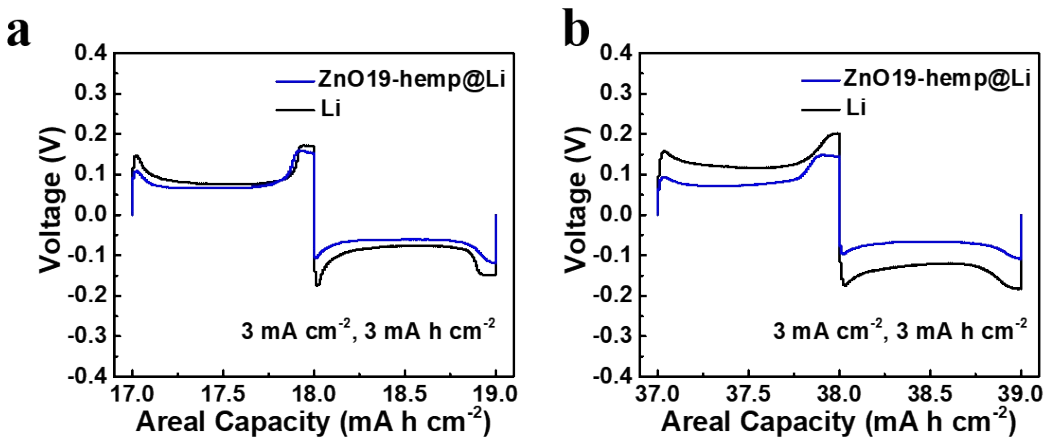

Fig. S7 Li plating and stripping profile of ZnO19-hemp@Li and pure Li chips at 3 mA cm^{-2} for 3 mA h cm^{-2}.

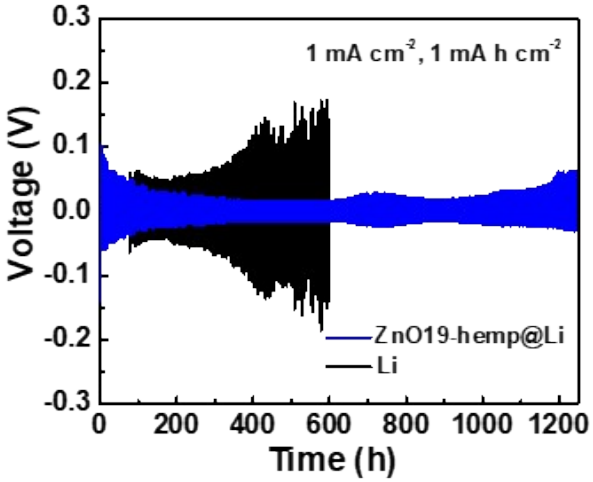

Fig. S8 Cycling stability of ZnO19-hemp@Li and Li in ether-based electrolyte at 1 mA cm^{-2} for 1 mA h cm^{-2}.

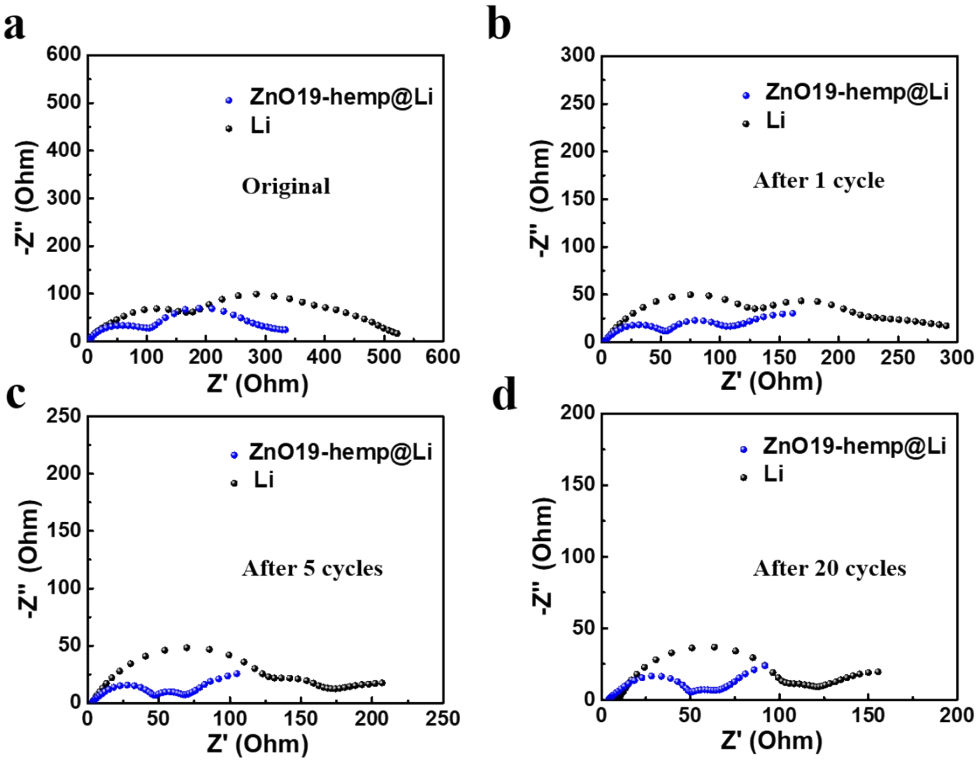

Fig. S9 EIS of ZnO19-hemp@Li and Li anodes (a) before cycles and after (b) 1 cycle, (c) 5 cycles and (d) 20 cycles at 1 mA cm^{-2} for 1 mA h cm^{-2}. According to the literatures, the semicircles at high frequency are believed to be associated with the charge transfer resistance. [1, 2]

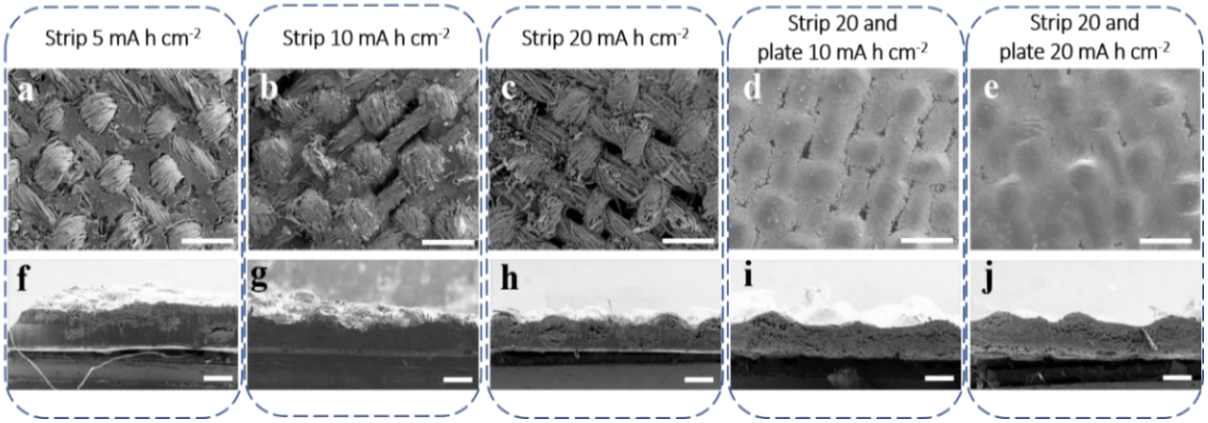

Fig. S10 Morphology of ZnO19-hemp@Li anodes. Top and cross section view of ZnO19-hemp@Li anodes after stripping 5 (a and f), 10 (b and g) and 20 (c and h) mA h cm^{-2} Li, followed by re-plating 10 (d and i) and 20 (e and j) mA h cm^{-2} after stripping 20 mA h cm^{-2}. Scale bar: 500 μm for Fig. 4a–d and 200 μm for Fig. 4f–j.

To elucidate the improved cycling stability and Li ion transfer kinetics, the morphological evolution of ZnO19-hemp@Li upon Li stripping and plating was observed by *ex-situ* SEM. Various amounts of Li were first stripped off and then re-deposited on ZnO19-hemp@Li at the current density of 1 mA cm^{-2} in carbonate electrolyte. As shown in Fig. 4a and f, when 5 mA h cm^{-2} Li was stripped, the surface Li close to the conductive hemp host was preferentially stripped off and the cross-sectional view shows negligible thickness variation. With the stripping capacity increased to 10 mA h cm^{-2}, more hemp fiber and void spaces were exposed (Fig. 4b) and the thickness of the electrodes reduced to ~220 μm (Fig. 4g). When 20 mA h cm^{-2} was Li stripped, the primary hemp fabric skeleton becomes obvious with most of the voids exposed, showing its structural integrity (Fig. 4c). The cross-section shows that the thickness of the electrode reduced to ~200 μm with more voids exposed (Fig. 4h). Subsequently, after 10 mA h cm^{-2} Li was re-plated back into the ZnO19-hemp@Li electrode after stripping 20 mA h cm^{-2} Li, the ZnO-hemp scaffold was preferentially covered by the deposited Li, leaving some voids within the woven structure (Fig. 4d). When 20 mA h cm^{-2} Li was fully re-deposited on the hemp matrix, the remaining voids and gaps between the fibers were filled, without sign of Li dendrite growth (Fig. 4e). After the plating process, the thickness of the electrodes was restored to ~240 μm (Fig. 4i–j), close to the original thickness of ZnO19-hemp@Li. In contrast, severe dendrite formation was observed when Li was deposited on a copper substrate (Fig. S11).

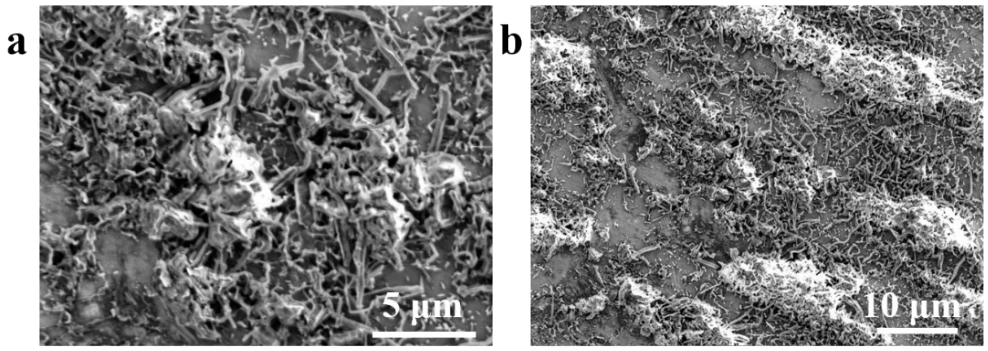

Fig. S11 SEM of 0.1 mA h cm^{-2} of Li deposited on copper substrate.

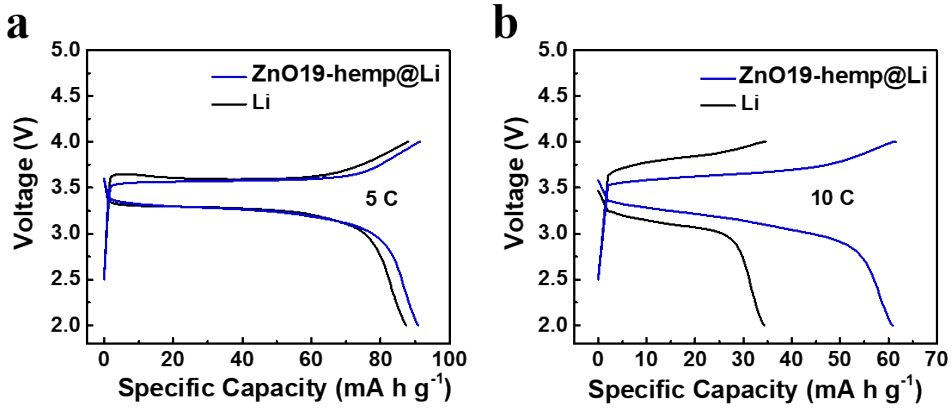

Fig. S12 Charge and discharge curves of LFP||ZnO19-hemp@Li and LFP||Li at (a) 5 C and (b) 10 C.

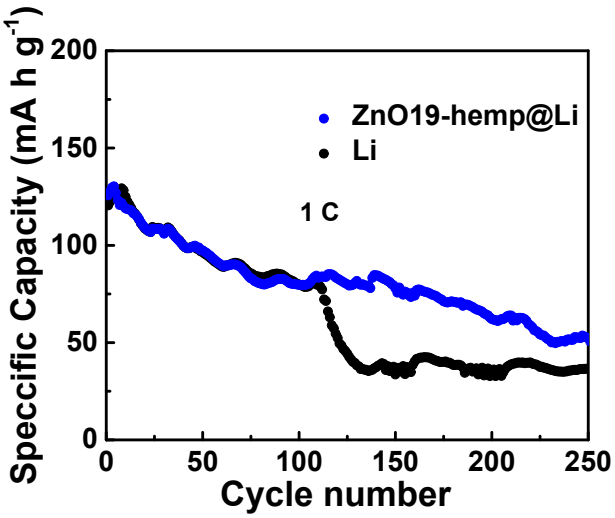

Fig. S13 Cycling performance of ZnO19-hemp@Li anodes (blue) and Li (black) in full cells with LFP (4 mA h cm^{-2}) as cathodes.

Table S1. Performance comparison of melt infused Li anodes in carbonate- and ether-based electrolytes

Materials	**Surface modification method**	**Thickness (μm)**	**Electrolyte**	**Current density (mA cm^{-2})**	**Cycling Capacity (mA h cm^{-2})**	**Cycle time (h)**	**Ref.**
Hemp derived carbon	Dip-coating	~240	1 M $LiPF_6$ in EC/DEC (1:1 vol %)	1 3 5 3	1 1 1 3	Over 400 Over 70 Over 50 Over 100	**This work**
			1 M LiTFSI in DOL/DME with 1% $LiNO_3$	1	1	Over 1200	
ZnO modified polyimide fiber	Atomic layer deposition	~253	1 M LiPF6 in EC/DEC (1:1 vol %)	1 3 5	1 1 1	Over 200 ~67 ~39	[3]
Nickle foam	None	~800	1 M LiPF6 in EC/DEC/EMC (1:1:1 vol %)	1 3 5	1 1 1	~200 ~67 ~40	[4]
ZnO modified wood	$Zn(NO_3)_2$ calcining at 400 °C	~500	1 M LiPF6 in EC/DEC (1:1 vol %)	1 3	1 1	~330 ~150	[5]
Ag modified carbon fiber	Electrodeposition	~150	1 M LiTFSI in DOL/DME with 2.0% $LiNO_3$	1 3	1 3	~400 ~160	[6]
CNT modified carbon cloth	Chemical vapor deposition	~360	1 M LiTFSI in DOL/DME with 1% $LiNO_3$	1	1	1000	[7]
$AuLi_3$ particles modified nickle foam	Electrodeposition	~500	1 M LiTFSI in DOL/DME with 1% $LiNO_3$	0.5 1	1 1	720 500	[8]
Co nanoparticles modified carbon nanofiber	Calcining	~93	1 M LiTFSI in DOL/DME with 2.0% $LiNO_3$	1	0.5	500	[9]

CRediT author statement

Zhiyu Wang: Investigation, Methodology, Writing – Original draft, Visualization

Peng Zhang: Resources, Investigation

Shasha Chen: Investigation

Ken Usman: Investigation

Dylan Hegh: Writing - Review & Editing

Robert Kerr: Methodology

Hongjie Zhang: Investigation, Funding acquisition, Project administration

Si Qin: Conceptualization, Investigation, Methodology, Writing – Original draft, Visualization, Supervision, Project administration

Chuyang Zhang: Funding acquisition, Supervision, Project administration

Dan Liu: Supervision, Writing - Review & Editing

Xungai Wang: Funding acquisition, Writing - Review & Editing

Weiwei Lei: Funding acquisition, Supervision, Writing - Review & Editing

Joselito M. Razal: Funding acquisition, Supervision, Project administration, Writing - Review & Editing

REFERENCES

1. S. S. Chi, Y. C. Liu, W. L. Song, L. Z. Fan and Q. Zhang, *Adv. Funct. Mater.*, 2017, **27**, 201700348.
2. H. S. Wang, X. Cao, H. K. Gu, Y. Y. Liu, Y. B. Li, Z. W. Zhang, W. Huang, H. X. Wang, J. Y. Wang, W. Xu, J. G. Zhang and Y. Cui, *Acs Nano*, 2020, **14**, 4601-4608.
3. Y. Liu, D. Lin, Z. Liang, J. Zhao, K. Yan and Y. Cui, *Nat. Commun.*, 2016, **7**, 10992.
4. S.-S. Chi, Y. Liu, W.-L. Song, L.-Z. Fan and Q. Zhang, *Adv. Funct. Mater.*, 2017, **27**, 1700348.
5. Y. Zhang, W. Luo, C. Wang, Y. Li, C. Chen, J. Song, J. Dai, E. M. Hitz, S. Xu, C. Yang, Y. Wang and L. Hu, *Proc. Natl. Acad. Sci. USA*, 2017, **114**, 3584-3589.
6. R. Zhang, X. Chen, X. Shen, X.-Q. Zhang, X.-R. Chen, X.-B. Cheng, C. Yan, C.-Z. Zhao and Q. Zhang, *Joule*, 2018, **2**, 764-777.
7. F. Liu, R. Xu, Z. Hu, S. Ye, S. Zeng, Y. Yao, S. Li and Y. Yu, *Small*, 2019, **15**, e1803734.
8. X. Ke, Y. Liang, L. Ou, H. Liu, Y. Chen, W. Wu, Y. Cheng, Z. Guo, Y. Lai, P. Liu and Z. Shi, *Energy Storage Mater.*, 2019, **23**, 547-555.
9. M. Shu, X. Li, L. Duan, M. Zhu and X. Xin, *Nanoscale*, 2020, **12**, 8819-8827.